GEOLOŠKI ANALI BALKANSKOGA POLUOSTRVA
Volume 86 (2), December 2025, 57-71
–
https://doi.org/10.2298/GABP251014011M
Original scientific paper
Оригинални научни рад

Mineralogical and structural characterization of zeolitic tuff from the Slanci deposit, Serbia

Katarina M. Mihajlović[1], Jovica Stojanović[2], Ana S. Radosavljević-Mihajlović[2], Ivana Jelić[2], Nikola Vuković[2], Slavica Mihajlović[2] & Vladan Kašić[2]

Abstract. Lake Miocene deposits located east of Belgrade in the Danube bend, around Veliko Selo and Slanci, are rich in zeolitic tuffs of the heulandite type. This paper presents mineralogical and structural investigations of zeolitic tuffs in which the dominant phase is Ca-heulandite with a Si/Al ratio of 3.78. Volcanic glass and biogenic amorphous silica are present as accompanying components. Quantitative X-ray powder analysis determined the following mineral composition: heulandite (85.1%), quartz (1.9%), muscovite (5.9%), albite (6.6%), orthoclase (0.6%) and calcite (0.21%). The structure was refined in the space group *C*2/*m*, with a disordered distribution of Al and Si within the tetrahedral framework. The following methods were applied: powder X-ray diffraction on a polycrystalline sample (XRPD), scanning electron microscopy and energy-dispersive X-ray spectroscopy (SEM/EDS), and differential thermal and thermogravimetric analysis (DTA/DTG/TG).

Key words:
Ca-heulandite, zeolitic tuff, Rietveld analysis, DTA/TG analysis.

Апстракт. Наслаге језерског миоцена које се налазе источно од Београда у Дунавском кључу, око Великог Села и Сланаца, богате су зеолитским туфовима хејландитског типа. У раду су представљена прегледна минералошка и структурна испитивања зеолитског туфа у којима је доминантна фаза Ca-хејландита са односом Si/Al 3.78. Вулканско стакло и биоегена аморфна силикатна маса су пратеће компоненте. Квантитативном рендгенском анализом утврђен је следећи минерални састав: хејландит (85.1 %), кварц (1.9 %), мусковит (5.9%), албит (6.6 %), ортоклас (0.6%) и калцит (0.21%). Структура је утачњавана у просторној групи *C*2/*m*, са неуређеном расподелом Al и Si у тетраедарској мрежи. За испитивање су коришћене методе рендгенске дифракције праха на поликристалном узорку (XRPD–X-Ray powder diffraction analysis), скенирајуће електронске микроскопије и енергодисперзивне спектроскопије X-зрацима (SEM/EDS, scanning electron microscopy and energy dispersive spectroscopy analysis) и диферцијално термичка и диферцијално термогравиметријска анализа (DTA/DTG, differential thermal and thermogravimetric analysis).

Кључне речи:
Ca-heulandite, зеолитски туф, Rietveld-анализа, DTA/TG анализа.

[1]University of Belgrade, Faculty of Mining and Geology, Đušina 7, 11000 Belgrade.
[2]Institute for Technology of Nuclear and Other Mineral Raw Materials, Franche d'Epere 86, 11000 Belgrade;
E-mail: a.radosavljevic@itnms.ac.rs

Introduction

Zeolites are specific tectosilicate structures in which (Si, Al)O_4 tetrahedra form a three-dimensional framework that creates cavities capable of hosting large cations and water molecules (Barrer, 1978; Armbrustr & Gunter, 2001). The general empirical composition can be expressed by the structural formula M_xD_y ($Alx_{+2y}Si_{n-(x+2y)}$) O_{2n}·mH_2O. The fundamental crystallochemical and structural features that define a zeolite species include the topological arrangement within the zeolitic cages, the symmetry of the space group, the Si^{4+}/Al^{3+} atomic ratio, dehydration processes, and the type and nature of cations in exchangeable positions (Combas et al., 1997; Armbrustr & Gunter, 2001; Bish, 1988). Due to their specific crystal structure, zeolites exhibit unique physicochemical properties that make them suitable for applications in various industrial sectors. Among the best-known members of this tectosilicate group are the zeolites belonging to the HEU series. The heulandite series (HEU) found in zeolitic tuff represents one of the most economically important groups of natural zeolites (Radosavljević-Mihajlović & Matović, 2008), with numerous applications in environmental and ecosystem-related processes (Vujaković et al., 2003; Radosavljević-Mihajlović et al., 2004; Lemić et al., 2006). Clinoptilolite and heulandite both belong to the HEU-type series of minerals, and due to the identical structural motif of their zeolitic frameworks, distinguishing between them can be challenging. According to the recommendations of the International Mineralogical Association, Commission on New Minerals and Mineral Names (Combas et al., 1997), heulandite is defined as the zeolite mineral series having the characteristic heulandite-type framework topology and a Si/Al ratio < 4, whereas clinoptilolite is defined as the corresponding series with the same framework topology but with a Si/Al > 4 (Combas et al., 1997). The genesis of zeolite deposits and the occurrence of zeolite-group minerals are associated with rocks of various types, ages, and origins. They most commonly occur in igneous, volcanogenic-sedimentary, and sedimentary rock complexes (Gottardi & Galli, 1985).

The genesis of Serbia's zeolitic tuffs, rich in minerals of the heulandite series, is associated with lacustrine and marine sedimentary deposits, where they formed through the devitrification of volcanic glass (Obradović, 1977). In these sedimentary rocks, zeolites occur as small crystals ranging from 0.1 to 100 μm, accompanied by other mineral components such as clay minerals and various aluminosilicate and silicate phases of similar densities. The subject of this study is the Late Miocene lacustrine deposits located east of Belgrade, within the Danube bend near Veliko Selo and Slanci. Zeolitic tuff occurs both at the surface in outcrops and in the subsurface, as confirmed by drilling. The general dip direction is west–southwest, 250/15–20–35°. The total thickness of the deposits identified to date is between 350 and 400 m, with the "Veliko Selo" and "Slanci" formations being of particular significance (Obradović & Dimitrijević, 1978; Stojanović et al., 2003; Kašić et al., 2014).

This paper presents the results of mineralogical and chemical investigations of the zeolitic tuff from the Slanci deposit. Structural parameters of the heulandite mineral present in the tuff are also reported. To support potential future applications of this raw mineral material, its thermal stability and ion-exchange properties were additionally examined.

Materials and Methods

The starting material for this study consisted of raw zeolitic tuff samples from the Slanci deposit, with a grain size of +100% −63 μm. Quantitative chemical analysis was performed using classical wet-chemical methods (Groves, 1951). To monitor the concentrations of exchangeable inorganic cations (Na^+, K^+, Ca^{2+}, and Mg^{2+}), the total cation-exchange capacity (CEC) was determined following the standard procedure of Ming & Dixon (1987). Qualitative mineralogical analysis was carried out using a polarization microscope ("JENAPOL-U" Carl Zeiss-Jena) in transmitted light on petrographic thin section. Objectives of 10–50× were used for mineral identification.

Powder X-ray diffraction (XRPD) analyses were performed using a "PW-1710" automatic powder diffractometer equipped with a Cu tube operating at 40 kV and 30 mA. A curved graphite monochro-

mator and a Xe scintillation counter were employed. Qualitative and structural XRPD analysis were conducted over the range 4–50° 2θ, with a time constant of 0.25 s and a step size of 0.02°. Quantitative phase analysis was performed using Siroquant V 4.0 software (Taylor, 1991). Structural refinements were carried out by the Rietveld method (Rietveld, 1969), implemented in the FullProf program (Rodriguez-Carvajal, 1990). Peak profiles were modeled using the pseudo-Voigt (pV) function. For thermally treated samples, diffractograms were recorded in the 2θ range 4–35° with a time constant of 0.5 s; for determination of structural parameters, measurements were made in the same 2θ interval with a time constant of 2.5 s and a step size of 0.02°. The resulting structural models were visualized using the crystallographic software VESTA (Momma & Izumi, 2011).

DTA/DTG/TG analyses were conducted in the temperature range 20–600 °C at a heating rate of 10 °C/min using a Netzsch STA-409 EP apparatus. Crystal morphology was examined by scanning electron microscopy (JEOL 840A). The samples were sputter-coated with gold using a JFC-1100 ion sputter.

Geology of the "Slanci" deposit

The wider Belgrade area represents an important geological unit covering approximately 2,000 km^2. It is situated within the contact zone between the southern margin of the Pannonian Basin and the inner Dinarides in the broader sense (Marinović & Rundić, 2020). The key Danube area near Belgrade is located at the boundary between the Balkan Mountains and the Pannonian Basin, on the southern bank of the Danube River, and includes the villages of Grocka, Višnjica, and Veliko Selo (Van der Made et al., 2007).

On the right bank of the Danube occur the oldest Neogene sediments, the "Slanci" series, which are rich in volcaniclastic material and contain numerous fossil remains (Dolić, 1997; Rundić et al., 2013; Knežević et al., 2015; Schwarchans et al., 2015). The first mammalian molar fossil from Miocene lacustrine sediments was discovered within the "Slanci Formation" (Van der Made et al., 2007). The broader area of investigation is composed of Lower and Middle Miocene sediments. The Middle Miocene is represented by marine Badenian and Sarmatian deposits (Stevanović, 1975; Mihajlović & Knežević, 1989). The marine Badenian deposits (Pannonian Sea–Paratethys) were deposited transgressively and discordantly over the lacustrine sediments of the "Slanci series." The Sarmatian deposits comprise older Sarmatian units made predominantly of clastic sediments (fossiliferous marls, marl clays, marl siltstones, sandy marls, etc.) (Mihajlović & Knežević, 1989). Quaternary deposits of various origins represent the youngest sedimentary unit in the Belgrade metropolitan area (Toljić et al., 2014). These formations cover Miocene sediments across most of the Belgrade Danube bend and include both Pleistocene and recent Holocene deposits.

Occurrences of tuffs within the Miocene sediments of the Belgrade Danube bend–especially in the so-called lacustrine "Slanci series" of the Lower (older) Miocene–have been described in the works of Stevanović & Stangačilović (1954), Stangačilović (1969), Stevanović (1975), Obradović (1977). According to Dolić (1997), three sedimentary units are distinguished: (a) the clastic formation of Veliko Selo (150–250 m thick), formed during the initial phase of the tectonic depression and the establishment of the former lake in which detrital material accumulated; (b) the "Slanci Formation," representing true lacustrine basin deposits—clays, laminated clayey marls, siltstones, sandstones, and clays with interbeds of tuffs and tuffites, as well as occurrences of coal and carbonaceous clays. According to Obradović (1980), the lamination indicates calm sedimentation conditions, while the occurrence of organic matter and plant remains reflects humid climatic conditions; (c) the youngest package of lacustrine deposits, represented by the clastic sediments of the so-called "Bučvar Formation," which vary significantly in thickness due to erosional removal in certain areas.

Research on zeolitic tuffs was conducted over an area of approximately 1.6 km^2 (the elevations of "Tapino brdo" and "Zapis," and the surrounding area near the village of Slanci) (Kondžulović et al., 2003; Kašić et al., 2004). Based on the investigations of Kašić et al. (2004), the ore-bearing zeolite layer in

this area has an average thickness of about 2.5 m (ranging from 1 to 3.9 m) and dips approximately 20° toward the north-northeast. The geological reserves amount to roughly 10,000 tons. However, the inclination of the ore layer (about 20°) is considered unfavorable from a mining perspective.

The method of constructing exploratory excavations is of great importance for planning and designing future work. The thickness of tuff interbeds does not exceed 2 m, while tuffite layers are somewhat thicker. The age of the main tuff interbed at the top of the "Slanci Formation" has been determined as Badenian, and the entire "Slanci Formation" is assigned to the Middle Miocene. While the beds at Veliko Selo are significantly disturbed (up to 35°), in the Slanci area the tuff interbeds are nearly horizontal. Based on the mode of occurrence (exclusively interbeds) and chemical composition, the tuffs correspond to synchronous dacitic tuffs from Fruška Gora, the Posavo–Tamnava region, central Šumadija, and the Morava Valley, and show no genetic relation to the older Tertiary intrusions on Avala (Kašić et al., 2004). Rich macroflora has been recorded within the zeolitic tuffs. Detailed examination by Dolić (1997) revealed the following: at a depth of 13.6 m, fossils of *Ostrea*, *Cardium*, and *Chlamys* were identified; at a depth of 119.9 m (marine Badenian), abundant marine fossils occur, including foraminifera, molluscs, and echinoids; at a depth of 129.8 m, freshwater fossil forms were found. The presence of echinoid remains was also confirmed within the zeolitic tuff in the study area (Figs. 1, 2).

These are fossilized remains of sea urchins (echinoids), spiny marine invertebrates that inhabit the seafloor. The area is also rich in macrofloral fossils discovered in gray marls, including *Cinnamomum*, *Myrica*, *Engelhartia*, and *Libocedrus*, indicative of warm-temperate climatic conditions, as well as *Populus*, *Salix*, *Zelkova*, and various ferns (Van der Made et al., 2007).

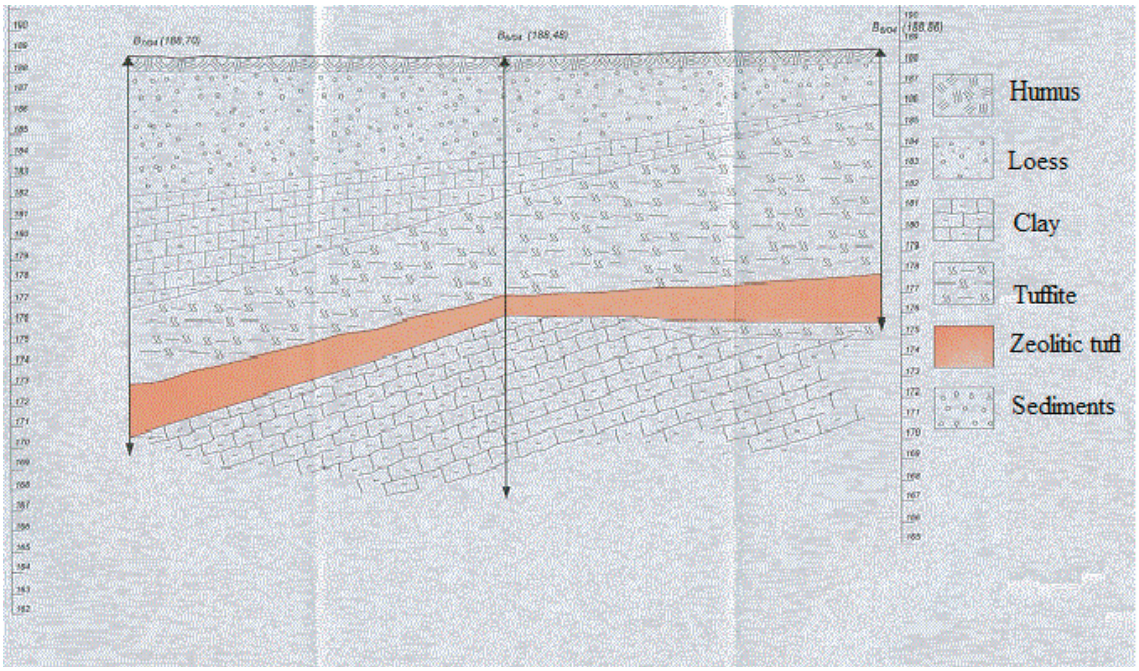

Fig. 1. *Characteristic geological profile of the "Slanci" zeolite deposit (Kašić et al., 2004).*

Result and disscusion

Mineralogical and chemical analysis of the Slanci zeolitic tuff

The groundmass of the sample is hypocrystalline, porphyritic to vitrophyric, and partially vesicular and porous. Quartz is almost always fresh, occurring in typical anhedral forms with sharp edges (Fig. 3a). Gas–liquid–solid inclusions are common. Rutile appears as solid inclusions within some grains. Several grains exhibit undulatory extinction, and their interference colors are gray to whitish of the first order.

Fig. 2. *Sea urchin of the genus Schizaster found in the "Slanci" zeolitic tuff (Photograph by the authors; the specimen is part of the collection of zeolitic tuffs housed at the Department of Applied Mineralogy and Crystallography, ITNMS).*

Feldspar minerals are predominated by plagioclase, which is largely altered—primarily sericitized and partly kaolinized (Fig. 3b). The preserved grains resemble quartz and contain numerous inclusions. Among the micas, biotite is the dominant primary mineral, whereas muscovite (sericite) occurs only as a secondary product (Fig. 3c).

Biotite is partially altered, mostly transformed into chlorite, and its alteration products include iron oxides and hydroxides (limonite–goethite). The pleochroic colors of preserved biotite range from light to dark brown, while chloritized biotite varies from brown-green to pale green. Anisotropy effects are subdued by its inherent coloration. Accessory minerals are typically fresh, transparent, and show no signs of alteration, most commonly appearing in tetragonal (zircon), prismatic (apatite; Fig. 3d), or acicu-lar (rutile) habits.

Zeolite minerals occur within the groundmass. They exhibit acicular habit and are very fine-grained. Anisotropy effects are visible, and interference colors range from gray to first-order white. Relatively frequent fossils, mostly of plant origin, are also observed within the groundmass. SEM micrographs of heulandite from the Slanci zeolitic tuff are shown in Fig. 4 (a–c).

In the central part of Figure 4c, well-developed crystal forms of heulandite can be observed, exhibiting a monoclinic ortho- prism with a front dome, clinopinacoid, and basal plane. The crystals reach sizes up to 15 μm (elongated along the b-axis). Other crystallographic combinations are also possible; however, monoclinic symmetry requires a single crystal for optical determination of crystal faces and corresponding interfacial angles. The mineral composition of the zeolitic tuff was additionally confirmed by powder X-ray diffraction on a polycrystalline sample (Fig. 5).

The following mineral composition was confirmed: heulandite, quartz, plagioclase, and amorphous material. Heulandite is the dominant mineral in the sample, whereas quartz and volcanic glass occur in significantly smaller quantities. Only negligible amounts of clay minerals, feldspars, and carbonates are present. Quantitative X-ray diffraction analysis identified the following phases in the Slanci sample:

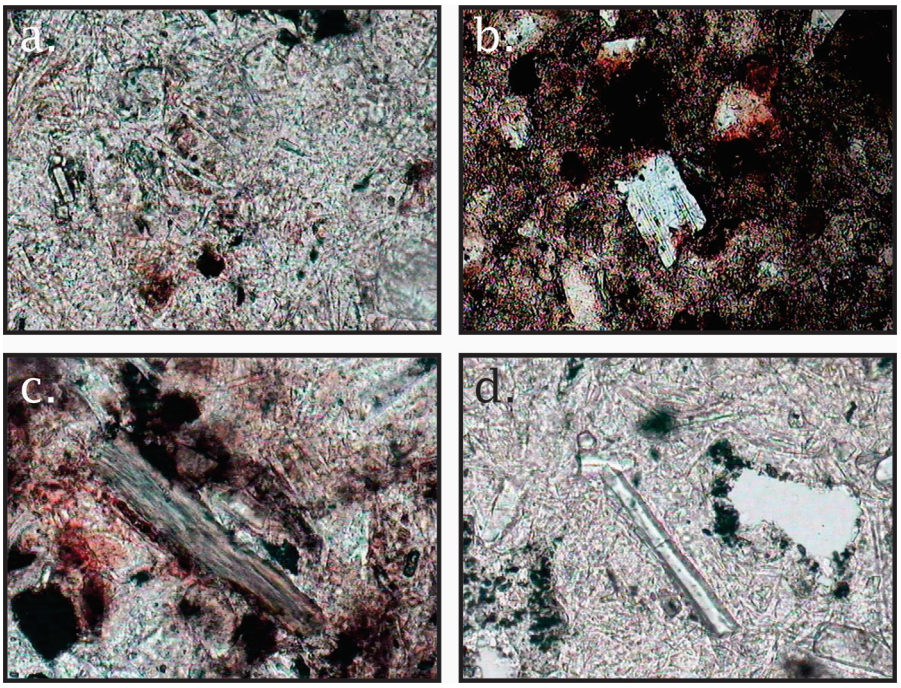

Fig. 3. ***a)*** *Quartz in the groundmass of the sample, objective 3.2×;* ***b)*** *Plagioclase in the sample, objective 10×;* ***c)*** *Biotite in the sample, objective 20×;* ***d)*** *Apatite crystal in the sample, objective 20×.*

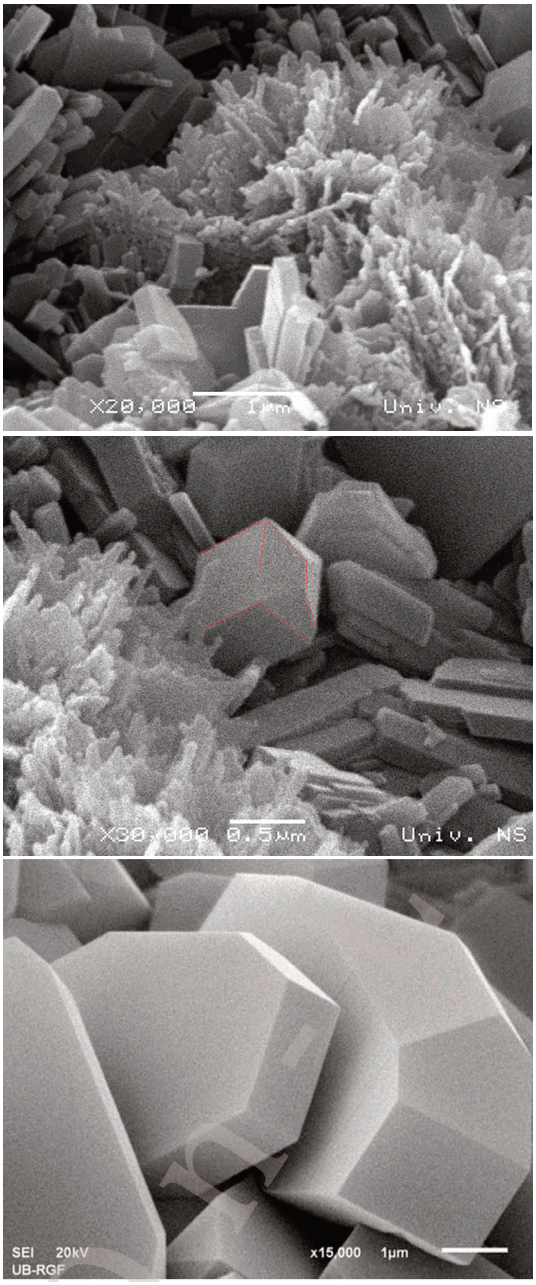

Fig. 4. *SEM micrographs of the heulandite mineral in the "Slanci" tuff:* ***a)*** *HEU mineral, scale bar 10 μm;* ***b)*** *Crystal forms of heulandite, scale bar 0.5 μm;* ***c)*** *Developed monoclinic forms of heulandite, scale bar 1 μm (15,000×).*

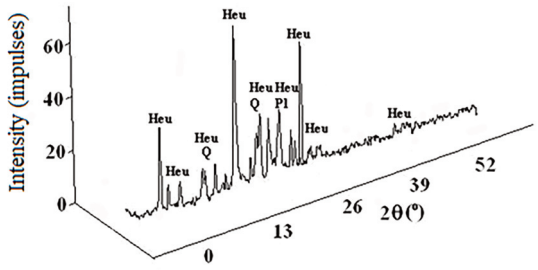

Fig. 5. *Powder X-ray diffractogram of the "Slanci" tuff (Heu–heulandite, Q–quartz, Pl–plagioclase).*

heulandite 85.1%, quartz 1.9%, muscovite 5.9%, albite 6.6%, orthoclase 0.6%, and calcite 0.21%.

Zeolitic tuffs are multiphase mixtures, and chemical analysis was performed on the bulk composition of the sample (Table 1). The analysis indicates a high silicon content, as well as the presence of oxides of alkali and alkaline-earth metals (Radosavljević-Mihajlović et al., 2005). The concentrations of heavy metals and exchangeable cations are also presented in Table 1.

The contents of Si and Al oxides in zeolitic tuffs from Serbian deposits are generally uniform, whereas the concentrations of oxides of monovalent and divalent cations vary among deposits. The highest Si/Al atomic ratio 4.70, has been recorded in the "Zlatokop tuff" (Radosavljević-Mihajlović et al., 2005). In the Slanci zeolitic tuff, the Si/Al atomic ratio is 3.78, and the proportion of divalent cations is higher than that of monovalent cations (Stojanović et al. 2003). As is well known, clinoptilolite and heulandite are distinguished on the basis of the Si/Al ratio; for clinoptilolite, Si/Al > 4, whereas for heulandite, Si/Al < 4 (Mason & Sand, 1960). Therefore, it can be concluded that the mineral present in the Slanci zeolitic tuff is Ca-heulandite, with calcium as the dominant extra-framework cation (Stojanović et al., 2003; Radosavljević-Mihajlović et al., 2005).

The presence of the heulandite mineral was also confirmed by thermal analysis. Mumpton (1960) defined clinoptilolite as the more thermally stable form, retaining its structure up to approximately 700 °C, whereas polymorphic transformations in heulandite begin at around 350 °C. Based on thermal analyses (thermal treatment of zeolitic tuff for 2 h at 350, 450, and 550 °C), the presence of a heulandite-type structure, specifically heulandite type I, was confirmed (Stojanović et al., 2003). Characteristic diffraction reflections were observed across the temperature range of 350–550 °C. Comparative X-ray powder diffraction diagrams of thermally treated zeolitic tuffs are presented in Fig. 6.

On the diffractogram at 550 °C (Fig. 6), heulandite reflections are still visible, although with very low intensity, and they are shifted toward higher 2θ angles. Crystallization of quartz is also observed, and at higher temperatures it remains the only crystalline phase present. Based on these results and the

Table 1. *Chemical composition, content of heavy metals and content of exchangeable cations in zeolitic tuff from the "Slanci" deposit.*

Chemical analsys of zeolitic tuff (content %)									
Oxide	SiO_2	Al_2O_3	Fe_2O_3	CaO	MgO	TiO_2	Na_2O	K_2O	G Ž
	60.94	16.08	1.72	4.72	0.78	0.17	0.26	0.63	12.65
Content of heavy metals in zeolitic tuff (ppm)									
Element	Cd	Cr	Ni	Pb	Cu	Zn	Mn		
	3.5	15.5	50	40	10	50	57		
Content of exchangeable cations in zeolitic tuff (MmolM+/100g)									
Ca^{2+}			Mg^{2+}		Na^+		K^+	CEC	
145			3.0		4.1		8.0	160.1	

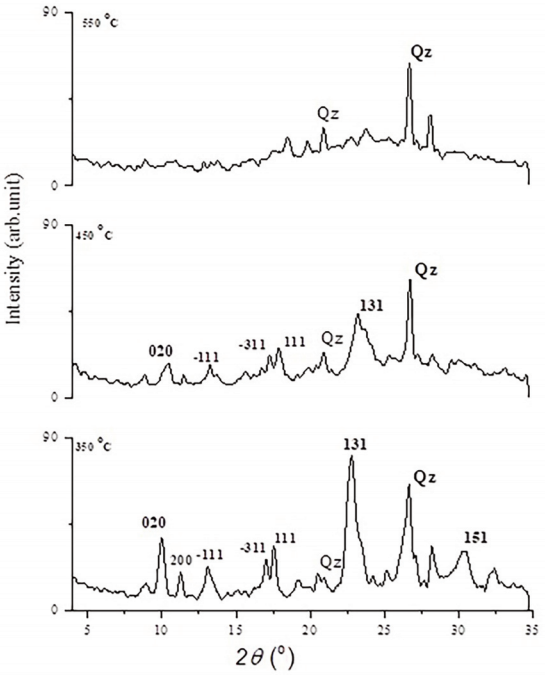

Fig. 6. *Comparative X-ray powder diffraction diffractograms of the "Slanci" tuff thermally treated at 350 °C, 450 °C and 550 °C.*

literature (Alberti, 1973), the observed phase can be classified as heulandite type I.

Structural analysis

A challenge in determining the structure of minerals present in zeolitic tuff is the multiphase nature of the samples. For structural refinement, the quantitative analysis must indicate more than 80% of the zeolite mineral. Amorphous and less stable components can be removed by NaOH treatment (Kokotailo & Fyfe, 1995). An advantage of the Rietveld refinement method is that it utilizes all points of the X-ray diffractogram and accounts for peak overlap (Rietveld, 1969). The presence of an amorphous phase does not interfere with refinement because the background arising from amorphous material is subtracted from the diffractogram baseline prior to refinement (Perdigão de Paiva et al., 2019). The crystal structure of heulandite is most commonly described as monoclinic, space group *C*2/*m* (Alberti, 1972; Armbruster & Gunter, 1991; Armbruster, 1993), reflecting a high degree of disorder in the distribution of tetrahedral Al/Si cations. Lowering of symmetry to *C*m or *C*1 may occur due to partial ordering of Al among the tetrahedral sites (Merkle & Slaughter, 1968; Yang & Armbruster, 1996). The crystallochemical composition of heulandites–particularly the type of dominant cation–is directly related to the unit-cell parameters. The unit-cell parameter values from the literature, along with those determined for the heulandite in the Slanci zeolitic tuff, are presented in Table 2. A comparative diagram illustrating the dependence of unit-cell parameters (a, b, c) on the proportions of monovalent and divalent cations is shown in Fig. 7.

Based on the comparative diagrams (Fig. 7a), an increased content of Ca^{2+} in the structure leads to an increase in the value of the *c* parameter, while the *a* and *b* parameters change more gradually. Likewise, an increase in the K^+ content (Fig. 7b) has the greatest effect on the crystallographic *c*-axis, producing an increase in its value. The heulandite from Slanci shows slight deviations from literature values, most likely due to the presence of different divalent and monovalent cations (Ca^{2+}, Mg^{2+}, Na^+, K^+) in its structure relative to published data.

Table 2. *The comparative values of the unit cell parameters of Ca-heulandite "Slanci" and data for various heulandites from the literature; a) Merkle & Slaughter, 1968; b) Alberti, 1973; c) Mortier & Pearce, 1981; d) Galli et al., 1983; e) Gunter et al., 1994; f) Khobaer et al., 2008)*

	Parameter of unite cell *a*, *b*, and *c* (Å); β (°); V (Å³) Space group *C*2/*m*				
Locality	***a***	***b***	***c***	**β**	**V**
Giebelsback, Switzerland[a] $Ca_{3.6}K_{0.8}Al_{8.8}Si_{27\ 4}$	17.73	17.82	7.43	116.3	2103.96
$Ca_{0.8}Na_{0.4}Al_2Si_7O_{18}$[b]	16.96	16.42	7.28	117.78	1792.64
Lane County, Oregon[c] $Na_{1.4}K_{0.1}Mg_{0.1}Ca_{3.3}Al_{8.3}Si_{27.7}O_{72}$	17.158	17.433	7.388	113.41	2027.96
Mossyrock Dam, Lewis Country Wachington, USA[d] $Na_{0.10}K_{8.57}Ba_{0.04}Al_9Si2_{27}$	17.767	17.958	7.431	115.93	2012.7
Poona,India[e] $Ca_{3.7}Na_{1.3}K_{0.1}A1_{8.9}Si_{27.1}O_{72}$	17.671	17.875	7.412	116.39	2097.24
Maharastra, India[f] $Na_{1.14}K_{0.40}Ca_{3.64}Sr_{0.21}Al_{9.21}Si_{26.88}$	17.716	17.880	7.438	116.43	2109.8
Slanci, Serbia $Ca_{1.45}Na_{0.11}Mg_{0.54}K_{1.05}Al_{7.4}Si_{28.4}O_{72}$	17.681	17.924	7.413	116.241	2117.406

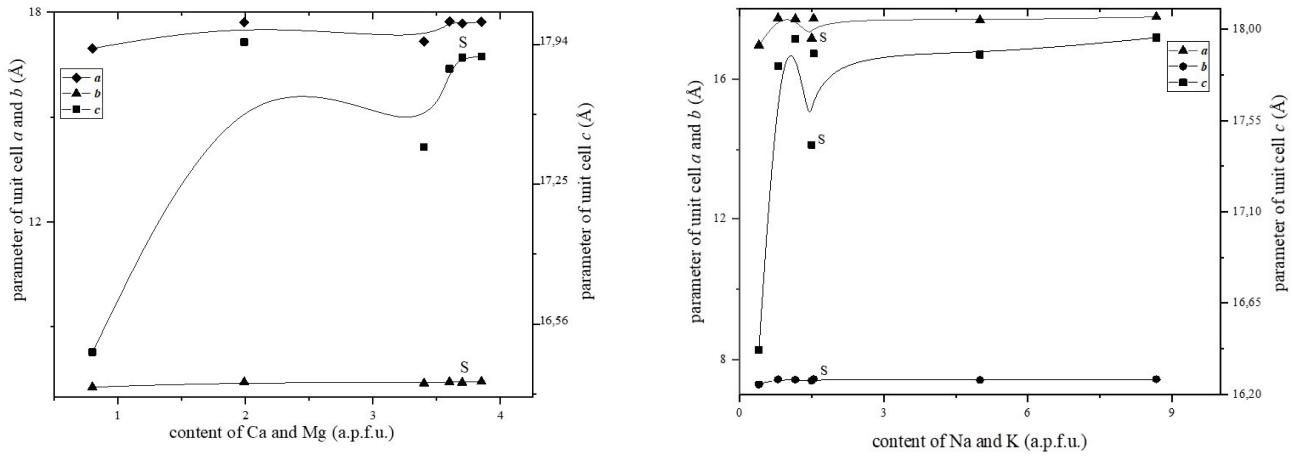

Fig. 7. *Comparative diagrams showing the dependence of unit cell parameters on the content of* ***(a)*** *divalent and* ***(b)*** *monovalent cations, based on Table 2.*

For the space group C2/m, it has been established that the tetrahedral site T2 can accommodate up to about 50% Al, whereas at the remaining positions T1, T4, and T5, the Al content does not exceed 25% (Koyama & Takeuchi, 1977). Four extra-framework cation positions have also been identified. Ca^{2+} cations occupying the M (I) position exert a strong attractive influence on the oxygen atoms of the tetrahedral framework, which in some structures results in channel narrowing (Gunter et al. 1994). The presence of K^+ in the M (III) position increases structural stability, while Ca^{2+} in M (I) does not produce significant changes (Gunter et al. 1994; Koyama & Takeuchi, 1977). The structure of Ca-heulandite from the Slanci zeolitic tuff was refined in the space group C2/m with a disordered distribution of Si and Al in the tetrahe-dral sites, as well as disordered occupancy of extra-framework cation positions within the zeolitic cages. The parameters from the KT model (Koyama & Takeuchi, 1977) were used as initial values. The refined powder X-ray pattern of Ca-heulandite is shown in Fig. 8, and the relevant structural and profile parameters, together with agreement factors, are given

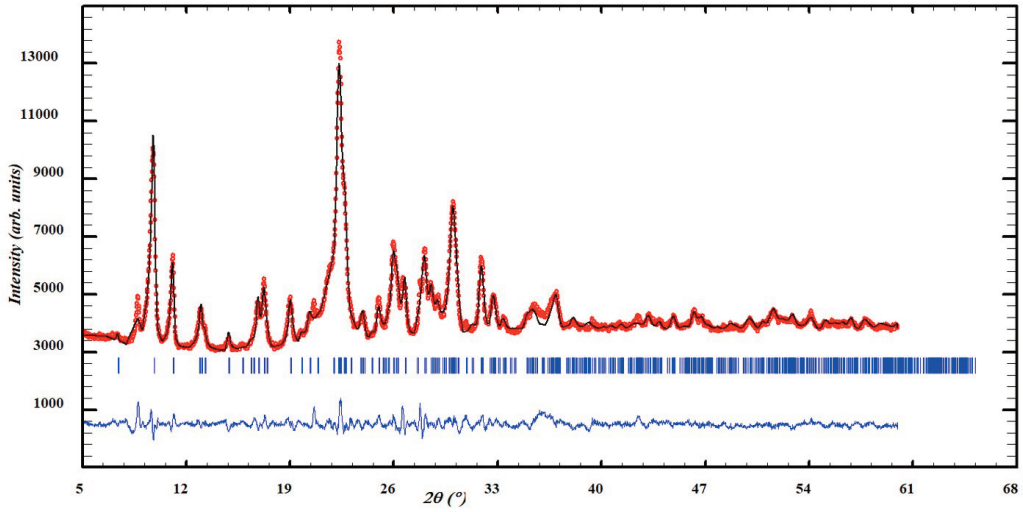

Fig. 8. *Observed (circles), calculated (solid line) and difference powder diffraction profiles for Ca-heulandite from "Slanci".*

in Table 3. Due to the structural complexity, isotropic displacement parameters were constrai-ned to be equal for atoms/ions of the same type. The refined fractional atomic coordinates, Wyckoff positions (W), and site-occupancy factors (SOF) for Ca-heulandite are listed in Table 4.

Table 3. *The relevant structural and profile parameters for Ca-heulandite "Slanci".*

Profile function	Pseudo-Voight
a (Å)	17.708 (3)
b (Å)	17.952 (3)
c (Å)	7.421 (3)
β (°)	116.177 (2)
V (Å³)/d (g/cm³)	2117.406 / 2.493
Space group	*C*2/*m*
2*θ* range (°)	5 - 60
Chi²	5.03
Rexp	2.14
Rwp	4.79
Rp	3.51
R(F)	20.1
R(B)	14.5

The basic structural framework consists of two channels parallel to the crystallographic *c*-axis (Fig. 9), designated A and B, each formed by ten tetrahedra arranged in rings.

In HEU-type minerals, five tetrahedral positions (T1–T5) are identified (Koyama & Takeuchi, 1977), of which four are occupied by SiO_4 groups, while AlO_4 occurs primarily at T2. Neglecting the influence of extra-framework cations, the ideal Si–O bond length in a TO_4 tetrahedron, based on Shannon radii, is ~1.61 Å, and the Al–O bond length is ~1.74 Å (for O^{2-} in II coordination) (Shannon& Prewitt, 1969). The presence of Al^{3+} in a tetrahedral site is indicated by increased T–O bond lengths; therefore, the greatest likelihood of Al^{3+} occupancy occurs at T2.

Table 4. *Refined framework fractional atomic coordinates, Wyckoff position (W) and site occupancy factor (SOF) of Ca-heulandite.*

Atom	*x*	*y*	*z*	SOF (Si/Al)
T1	0.177	0.170	0.105	0.7691/0.011
T2	0.213	0.414	0.502	0.789/0.187
T3	0.206	0.190	0.707	0.768/0.187
T4	0.074	0.303	0.433	0.77/0.187
T5	0.0	0.225	0.0	0.29/0.187
O1	0.194	0.5	0.46	1
O2	0.231	0.12	0.606	1
O3	0.165	0.154	0.868	1
O4	0.231	0.009	0.243	1
O5	0.0	0.33	0.5	1
O6	0.074	0.163	0.048	1
O7	0.118	0.231	0.562	1
O8	0.014	0.275	0.203	1
O9	0.207	0.255	0.173	1
O10	0.123	0.371	0416	1

In Ca-heulandite from Slanci, the longest Si, Al–O bond lengths are observed at positions T1, T3, and T5. These deviations from the KT model (Koyama & Takeuchi, 1977) stem from the influence of Ca^{2+} as an extra-framework cation. Ca^{2+} has been shown to distort the tetrahedral framework (Mortier & Pearce, 1981). Calcium occupies the M (I) and M (II) positions within the eight-membered ring, with M (II) showing particularly strong affinity for frame-

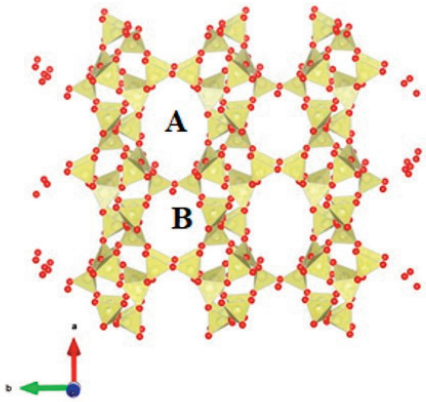

Fig. 9. *Projection of the structure of Ca-heulandite ("Slanci") along the crystallographic plane a/b. Channels of 10-membered (10 mR) and 8-membered (8 mR).*

Table 5. *The distances of bond lengths <T–O > and <M–O> in the structure of Ca-heulandite "Slanci".*

<T–O>[Å]		<M–O> [Å]	
T1 – O	1.663	M (I) – O	3.05
T2 – O	1.632	M (II) – O	2.617
T3 – O	1.651	M (III) – O	2.975
T4 – O	1.602	M (IV) – O	3.20
T5 – O	1.715	M – O	2.960
T – O	1.637		

work oxygen (Fig. 12). This interaction leads to distortion of the tetrahedral network and a reduction in channel opening sizes. The positions and occupancy factors of extra-framework cations and water molecules in Ca-heulandite from Slanci are presented in Table 6.

Table 6. *Refined framework fractional atomic coordinates, Wick-off position (W) and site occupancy factor (SOF) for extrafarmework cations and water molecules of Ca-heulandite "Slanci".*

Atom	W.	*x*	*y*	*z*	SOF
Na1(I)	4*i*	0.2845	0.0	-0.03	0.154
Ca1 (I)	4*i*	0.2845	0.0	-0.03	0.279
Ca2 (II)	4*i*	0.027	0.5	0.187	0.209
K (III)	4*i*	0.264	0.0	-0.059	0.351
Mg (IV)	2*c*	0.0	0.0	0.5	0.013
Ow_1	4*i*	0.242	0.0	0.114	0.34
Ow_2	4*i*	0.109	0.0	0.936	0.15
Ow_3	8*j*	0.074	0.425	0.973	1
Ow_4	2*d*	0.5	0.0	0.5	0.25
Ow_5	8*j*	0.028	0.066	0.373	0.5
Ow_6	4*i*	0.047	0.0	0.17	0.25
Ow_7	4*i*	0.09	0.0	0.631	0.25
Ow_8	4*i*	0.0083	0.0	0.083	0.25
Ow_9	4*i*	0.109	0.0	0.589	0.25
Ow_{10}	4*i*	0.042	0.0	0.767	0.13

All cations are located at 4i positions on the mirror plane. Two cation sites are present in channel A: M (I) and M (IV). The M (I) position is

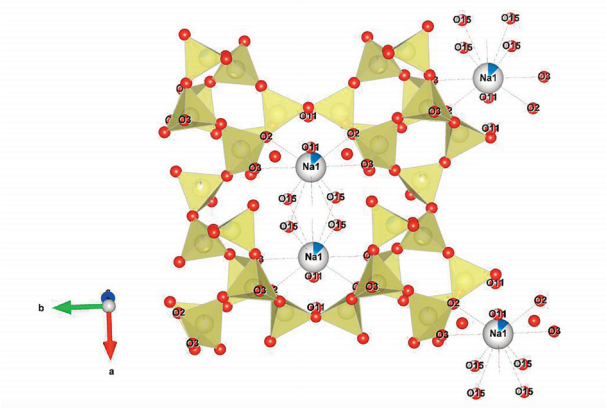

Fig. 10. *Position of the M (I) cation, (Ca/Na) within the tetrahedral network/ channel A.*

coordinated to four oxygen atoms and five water molecules; Na^+ and Ca^{2+} both show strong affinity for this site (Fig. 10). The coordination number is CN = 9, with an average bond length of 3.05 Å (four O atoms at 3.18 Å and five H_2O molecules at 2.92 Å), as shown in Fig. 11.

In channel B, the cation position M (II) is present, where cations are coordinated to three oxygen atoms and five water molecules, resulting in a coordination CN=8, (Fig. 12). It has been demonstrated

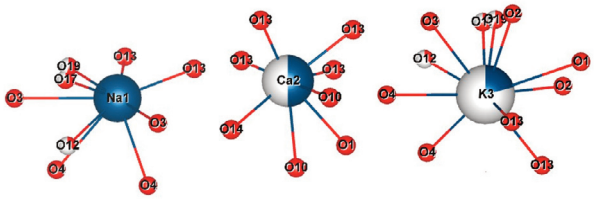

Fig. 11. *Coordination polyhedron around Na, Ca and K atoms, in the extrafamework positions M (I), M (II) and M (III).*

that Ca^{2+} shows a greater affinity than Na^+ for this position (Koyama & Takeuchi, 1977). The Ca (II) site is eightfold coordinated with three O atoms (2×O10 and O1) in the tetrahedral framework, and five fully occupied H_2O molecules, with an average connection length of 2.617 Å (Fig. 12).

Based on the cation exchange capacity results (Tab. 1), the structure of Ca-heulandite contains 145 *meq* Ca (0.437 apfu) and 4.1 *meq* Na (0.024 apfu), suggesting that Ca atoms are distributed in both M (I) and M (II) positions. This distribution contributes to the stability of the structure. At the center of the eight-membered ring, there is the cation

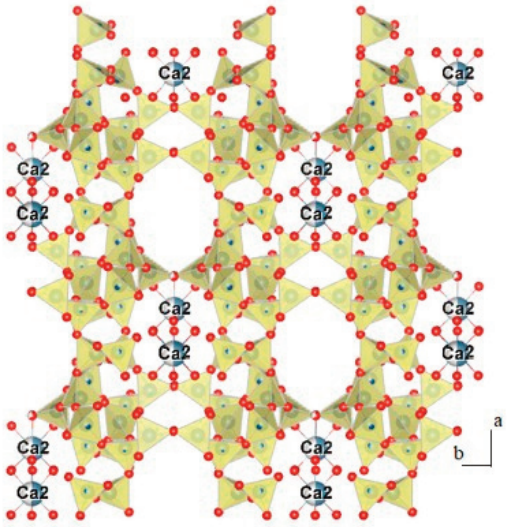

***Fig. 12**. Position of extrafarmework cation M (II) – Ca (II) in channel B.*

position M (III), in channel C. The K^+ ion occupies this position and, according to literature data, is coordinated to six oxygen atoms from the framework and three water molecules (CN=9). In Ca-heulandite, the K atom is coordinated to four oxygen atoms from a tetrahedral network (average bond length 3.12 Å) and five water molecules (average bond length 2.83 Å) (Fig. 13). The observed differences are likely due to the presence of the Ca cation, which causes distortions in the tetrahedral network.

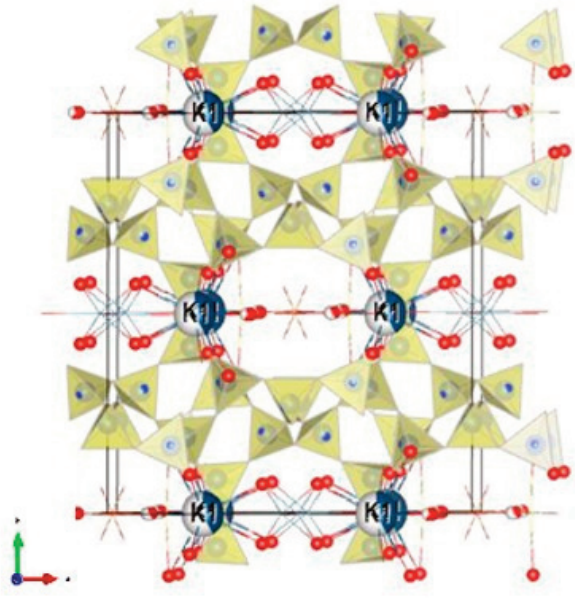

***Fig. 13.** Position of extrafarmework cation M (III) – K in channel B.*

The stability of channel C is enhanced by the presence of K^+ in this position, thereby increasing the overall stability of the structure (Koyama & Takeuchi, 1977). Previous research (Stojanović et al., 2003; Kašić et al., 2014; Radosavljević-Mihajlović et al., 2003, 2005, 2018) has determined that Ca–clinoptilolites from zeolitic tuffs in Zlatokop, Novakovići, and Beočin contain approximately 30 meq K^+ in exchangeable positions (0.181 atoms/mol). Thermal treatment has confirmed their stability up to 700 °C. The thermal stability of zeolite tuff "Slanci" (550 °C) (Stojanović et al., 2003) is the lowest, likely due to the K^+ content in the structure (0.048 atoms/mol).

Thermal analyses

Thermal analysis (DTA/DTG/TG) provides significant information on the processes of dehydration, dehydroxylation, and thermal stability of zeolitic tuffs. It has been established that the differences arising during thermal treatment are a function of the crystallochemical composition, i.e., the type and content of extraframework cations, as well as the framework cations Si and Al (Alberti & Vezzalini, 1983; Bish, 1984, 1990; Bish & Duffy, 1990; Bish & Carey, 2001). The results of differential thermal and thermogravimetric analysis are presented in Fig. 14.

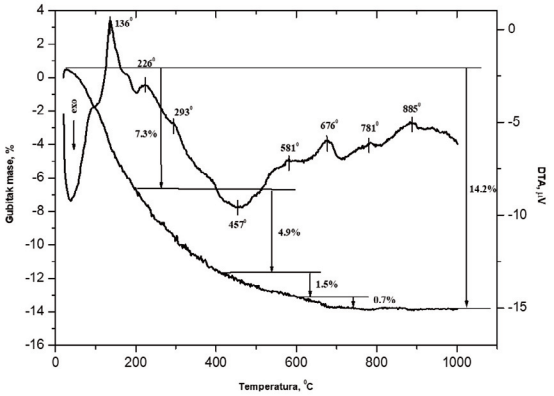

***Fig. 14.** DTA/DTG/TG effects of "Slanci" zeolitic tuffs.*

The DTA effects observed in the diagram (Fig. 14) are a consequence of desorption and dehydration processes of water present in the zeolite structure (Alberti & Vezzalini 1983; Bish, 1984; Bish & Duffy, 1990). Water in the zeolitic cages is bound by weaker or stronger interactions to different extraframework cations. According to the described KT

model (Koyama & Takeuchi, 1977), ten water molecules are coordinatively bound to cations (Ca^{2+}, Mg^{2+}, Na^{+}, K^{+}), which can occupy four cation positions [M (I), M (II), M (III), and M (IV)]. The most weakly bound water coordinated to cations in positions M (I) and M (IV) in channel A leaves the channels first. On the DTA diagram, this dehydration process is characterized by the first wide endothermic peak in the temperature interval of 50–200°C, where two endothermic effects occur: the first, more pronounced at 136 °C, and the second, less pronounced at 226°C. A third, less pronounced endothermic effect occurs at 293 °C and results from water release from channel B, where it forms a stronger bond with Ca cations in position M (II) (Fig. 12).

In the temperature range of 450–885°C (462 °C, Fig. 7), endothermic effects correspond to water bound to the K cation in position M (III) (Fig. 13), as well as to dehydroxylation processes. The DTA diagram (Fig. 14) also shows an endothermic effect at 676 °C, which most likely corresponds to organocarbonates present in this zeolite sample (biological material in the form of fossils). This peak is also characteristic of the zeolitic tuff from the Beočin deposit, which contains fossil remains (Radosavljević-Mihajlović et al. 2003; Kašić et al. 2004). The measured total weight loss (14.2%) is in good agreement with the calculated (12.65%). Most of the water (7.3% of the total weight) is continuously lost at temperatures below approximately 250°C, and then part of the remaining 7.1% is slowly dehydrated up to 650°C, with complete dehydration of the sample achieved at 885 °C.

Conclusion

Based on the presented results, it can be concluded that the zeolitic tuff contains 85% of the mineral heulandite (HEU), with calcium (Ca) as the dominant cation. Chemical and thermal analyses, along with X-ray powder diffraction on a polycrystalline sample, confirmed the presence of Ca-heulandite. The structure of Ca-heulandite was determined to belong to the centrosymmetric space group C2/m, with unit cell parameters of a = 17.662 Å, b = 17.874 Å, c = 7.402 Å, β = 116.32°, V = 2122.73 $Å^3$, and a density of ρ = 2.570 g/cm^3. The total cation exchange capacity is 160.1 Mmol M^+/100g, which indicates exceptional potential for absorption processes and various chemical applications. The zeolitic tuff exhibits thermal and structural stability, suggesting its applicability in diverse fields of industry and agriculture.

Acknowledgement

The authors acknowledge the support of the Ministry of Education, Science and Technological Development of the Republic of Serbia for funding the research through the project (numbre of contract 451-03-136/2025-03/200023). The authors would like to express special gratitude for the advice and help in the preparation of the paper, Prof. Slobodan A. Radosavljević. Also, the authors would like to thank Prof. Vesna Rakić and an anonymous reviewer for their constructive comments, which greatly improved the manuscript

References

Alberti, A. 1972. On the crystal structure of the zeolite heulandite. *Tschermaks Mineral. Petrogr. Mitt.*, 18: 29–146.

Alberti, A. 1973. The structure of heulandite B. *Tschermaks Mineral. Petrogr. Mitt.*, 19: 173–184.

Alberti, A. & Vezzalini, G. 1983. The thermal behavior of heulandites: A structural study of the dehydration of the Nadap heulandite. *Tschermaks Mineral. Petrogr. Mitt.*, 31: 259–270.

Armbruster, T. 1993. Dehydration mechanism of clinoptilolite and heulandite: Single-crystal X-ray study of Na-poor, Ca-, K-, Mg-rich clinoptilolite at 100 K. *Am. Mineral.*, 78: 260–264.

Armbruster, T. & Gunter, M.E. 1991. Stepwise dehydration of heulandite-clinoptilolite from Succor Creek, Oregon, USA: A single-crystal X-ray study at 100 K. *Am. Mineral.*, 76: 1872–1883.

Armbrustr, T. & Gunter, M. 2001. Crystal structures of Natural Zeolites. In: Bish, D. & Ming, D. (Eds.). *Natural Zeolites: Occurrence, Properties, Applications*. Reviews in mineralogy and geochemistry, 45: 1–67.

Barrer, R.M. 1978. *Zeolites and Clay Minerals as Sorbents and Molecular Sieves*. Academic Press, London-New York, 45 pp.

Bish, D.L. 1984. Effects of Exchangeable Cation Composition on the Thermal Expansion/ Contraction of Clinoptilolite. *Clays and Clay Minerals*, 32: 444–452.

Bish, D.L. 1988. Occurrence, Properties and Utilization of Natural Zeolites. In: Kallo, D. & Sherry, H.S. (Eds.). *Proceedings of the Second International Conference on the Occurrence, Properties and Utilization of Natural Zeolites in 1988*, Akademiai Kiado, Budapest, 565–576.

Bish, D.L. 1990. Long-term thermal stability of clinoptilolite: The development of a "B" phase. *Eur. J. Mineral*., 2: 771–777.

Bish, D. & Carey, W. 2001. Thermal behavior of Natural Zeolites. In: Bish, D. & Ming, D. (Eds.). *Natural Zeolites: Occurrence, Properties, Applications*. Reviews in mineralogy and geochemistry, 45: 403–452.

Bish, D.L. & Duffy, C.J. 1990. Thermogravimetric Analysis of Minerals. *Thermal Analysis in Clay Science*, 96–157.

Coombs, D.S., Alberti, A., Armbruster, T., Artioli, G., Colella, C., Galli, E., Grice, J.D., Liebau, F., Mandarino, J.A., Minato, H., Nickel, E.H., Passaglia, E., Peacor, D.R., Quartieri, S., Rinaldi, R., Ross, M., Sheppard, R.A., Tillmanns, E., & Vezzalini, G. 1997. Recommended nomenclature for zeolite minerals: Report of the Subcommittee on Zeolites of the International Mineralogical Association, Commission on New Minerals and Mineral Names. *Can. Mineral.,* 35: 1571–1606.

Dolić, D. 1997. Jezerski miocen kod Beograda [Lacustrine Miocene near Belgrade – in Serbian]. *Geološki Anali Balkanskog Poluostrva*, 61 (2): 15–32.

Galli, G., Gottardi, G., Mayer, H., Preisinger, A. & Passaglia, E. 1983. The structure of potassium-exchanged heulandite at 293, 373 and 593 K. *Acta Cryst. Section B*, 39 (2): 189–197.

Gottardi, G. & Galli, E. 1985. *Natural Zeolites*. Springer-Verlag, Berlin, 78pp.

Groves, A.W. 1951. *Silicate analysis. A manual for geologists and chemists with chapters on check calculations and geochemical data*. 2nd edition. George Allen & Unwin Ltd. London, 336pp.

Gunter, M., Armbruster, T., Kohler, Th. & Knowles, C. 1994. Crystal structure and optical properties of Na- and Pb-exchange heulandite-group zeolites. *American Mineralogist*, 79: 675–682.

Kašić, V., Životić, D., Simić, V., Stojanović, J., Radosavljević-Mihajlović, S.A., Sekulić, Ž. & Mihajlović, S. 2014. Geology of the Slanci zeolitic tuff deposit near Belgrade (Serbia). *9th International Conference on Occurrence, Properties and Utilization of Natural Zeolites, Beograd*, 105–107.

Kašić, V., Radosavljević, S., Stojanović, J. & Radosavljević-Mihajlović, S.A. 2004. Godišnji izveštaj o izvršenim radovima po projektu geoloških istraživanja zeolitskih tufova kod sela Slanci u Beogradskom dunavskom ključu [Annual report on the work carried out under the geological research project of zeolitic tuffs near the village of Slanci in the Belgrade Danube Gate – in Serbian]. *ITNMS*, 1–26.

Khobaer, T., Kuribayashi, T., Komatsu, K. & Kudoh, Y. 2008. The partially dehydrated structure of natural heulandite: An situ high temperature single crystal X ray diffraction study. *Journal of Mineralogical and Petrological Sciences*, 103: 61–76.

Knežević, S. & Krstić, N. 2015. Slanačka serija na zapadu Beograda, u dedinjskom saobraćajnom tunelu [Slanci series west of Belgrade, in the Dedinje traffic tunnel – in Serbian]. Zapisnici SGD za 2014, 25–32.

Kokotailo, G.T. & Fyfe, C.A. 1995. Zeolite structure analysis with powder x-ray diffraction and solid-state NMR techniques. *The Rigaku Journal*, 12 (1): 3–10.

Kondžulović, R., Nikolić, M. & Knežević, S. 2003. Projekat geoloških istraživanja zeolitskih tufova kod sela Slanci u Beogradskom Dunavskom Ključu [Geological research project of zeolitic tuffs near the village of Slanci in the Belgrade Danube Gate – in Serbian]. Unpublished report, 1–20.

Koyama, K. & Takeuchi, Y. 1977. Clinoptilolite: The distribution of potassium atoms and its role in thermal stability. *Zeitschrift für Kristallographie*, 145: 216–239.

Lemić, J., Milošević, S., Vukašinović, M., Radosavljević-Mihajlović, A. & Kovačević, D. 2006. Surface modification of a zeolite and the infliuence of pH and ionic strenngth on the desorption of an amine. *Journal of the Serbian Chemical Society*, 71 (11): 1161–1172.

Marinović, Đ. & Rundić, Lj. 2020. Depth geological relations of the wider area of Belgrade-based on the wells and geophysical data. *Geološki anali Balkanskoga poluostrva*, 81: 1–32.

Mason, B. & Sand, L.B. 1960. Clinoptilolite from Patagonia: The relationship between clinoptilolite and heulandite. *American Mineralogist*, 45: 341–350.

Merkle, A.B. & Slaughter, M. 1968. Determination and refinement of the structure of heulandite. *Am Mineral.*, 53: 1120–1138.

Mihajlović, Đ. & Knežević, S. 1989. Krečnjački nanoplank-ton iz badenskih i sarmatskih naslaga Višnjice i Karaburme (Beograd) [Calcareous nannoplankton from the Badenian and Sarmatian deposits at Višnjica and Karaburma in Belgrade – in Serbian]. *Geološki anali Balkan- skoga poluostrva*, 63: 373–383.

Ming, D.W. & Dixon, J.B. 1987. Quantitative determination of clinoptilolite in soils by a cation-exchange capacity method. *Clays Clay Miner*., 35 (1): 463–468.

Momma, K. & Izumi, F. 2011. VESTA 3 for three-dimensional visualization of crystal, volumetric and morphology data. *J Appl. Crystallography*., 44: 1272–1276.

Mortier, W. & Pearce, J. 1981. Thermal stability of the heulandite-type framework: crystal structure of the calcium/ammonium form dehydrated 483K. *American Mineralogist*, 66: 309–314.

Mumpton, F.A. 1960. Clinoptilolite redefined. *American Mineralogist*, 45: 351–36.

Obradović, J. 1977. The review on the occurrence of zeolites in sedimentary rocks in Yugoslavia. *Geološki anali Balkanskoga poluostrva*, 41: 293–302.

Obradović, J. 1980. Sedimentološka ispitivanja uzoraka iz bušotina Višnjica–Veliko selo [Sedimentological investigations of samples from the Višnjica–Veliko Selo bore-holes – in Serbian]. *Elaborat Kosovoprojekt, Fond Sekretarijata za urbanizam, Beograd*, 1–20.

Obradović, J. & Dimitrijević, R. 1978. The Pyroclastic rocks with analcime from Slanci series of the Danube River bend near Belgrade. *Geološki anali Balkanskoga poluostrva*, 42: 483–494.

Perdigão de Paiva, P.R., Ferreira, A.M., Silva, G.C., Teixeira Ciminelli, V.S. & Weidler, P.G. 2019. Evaluation of the Rietveld method for the mineralogical characterization of airborne dust in a mining area, Mining. *REM, Int. Eng. J.*, 72 (2): 329–334.

Radosavljević-Mihajlović, A., Daković, A., Kašić, V., Mitić, V., Stojanović, J., Sokić, M. & Marković, M. 2018. Mineralogy and crystallographic properties of Heu-type zeolitic tuff from the Novaković deposit, Bosnia and Herzegovina. *Hemijska industrija,* 72 (6): 371–382.

Radosavljević-Mihajlović, S.A., Dondur, V., Daković, A., Lemić, J. & Tomašević-Čanović, M. 2004. Physicochemical and structural characteristics of HEU-type zeolitic tuff treated by hydrochloric acid. *Journal of the Serbian Chemical Society,* 64 (4): 273–282.

Radosavljević-Mihajlović, S.A. & Matović, B. 2008. Prirodni zeoliti i mogućnost njegove primene u zaštiti životne sredine [Natural zeolites and the possibilities of their application in environmental protection – in Serbian]. *NBP, Nauka, Tehnika, bezbednost,* 8 (2): 107–119.

Radosavljević-Mihajlović, S.A., Stojanović, J. & Kašić, V. 2005. Uporedne mineraloške, kristalohemijske i termičke osobine ležišta zeolitskih tufova Srbije bogatih mineralima HEU-tipa [Comparative mineralogical, crystallo-chemical, and thermal properties of HEU-type mineral–rich zeolitic tuff deposits of Serbia – in Serbian]. *Radovi Geoinstituta*, 40: 191–200.

Radosavljević-Mihajlović, A., Stojanović, J., Kašić, V. & Lemić, J. 2003. Mineralogy and crystal chemistry of zeolitic tuffs from three deposits: Zlatokop, Beočin and Novakovići. *Bulletin of Geoinstitute*, 38: 149–155.

Rietveld, H.M. 1969. A profile refinement method for nuclear and magnetic structures. *J. Appl. Crystal*., 2: 65–71.

Rodriguez-Carvajal, J. 1990. Fullprof: A Program for Rietveld Refinement and Pattern Matching Analysis. *Abstract of the Satellite Meeting on Powder Diffraction of the XV Congress of the IUCr, Toulouse, France*, 127.

Rundić, Lj., Dolić, D. & Knežević, S. 2013. Continental-Lacustrine Lower Miocene of the Belgrade City area (Serbia): state of art. *Proceedings of the 5th Intern. Workshop on Neogene of Central and SE Europe, Varna,* 55.

Schwarchans, W., Bradić, K. & Rundić, Lj. 2015. Fish-otoliths from the marine-brackish water transition from the Middle Miocene of the Belgrade area, Serbia. *Paläontologische Zeitschrift,* 89 (4): 815–837.

Shannon, R.D. & Prewitt, C.T. 1969. Effective ionic radii in oxides and fluorides. *Acta Crystall*., B25: 925–945.

Stangačilović, D. 1969. Submarinski vulkanizam u tortonu Beogradskog Dunavskog ključa. [Submarine volcanism in the Tortonian of the Belgrade Danube Cape – in Serbian]. *Zapisnici SGD za 1964*, 233–238.

Stevanović, P. & Stangačilović, D. 1954. O pojavama vulkanskog tufa u miocenskim naslagama Beogradskog dunavskog ključa [On occurrences of volcanic tuff in the Miocene deposits of the Belgrade Danube Gate – in Serbian]. *Zapisnici SGD za 1950, 1951, 1952. godinu*, 67–78.

Stevanović, P. 1975. Stratigrafski položaj tercijarnih eruptivnih u okolini Beograda, Vulkanizam Beogradskog dunavskog ključa [Stratigraphic position of the Ter-

tiary eruptions in the area of Belgrade, Volcanism of the Belgrade Danube Gate – in Serbian]. *Acta geologica*, 8: 456–459.

Stojanović, J. Radosavljević-Mihajlović, S.A. & Kašić, V. 2003. Prilog poznavanju zeolitskog tufa sa lokalnosti Slanci, kod Beograda [Contribution to the knowledge of zeolitic tuff from the Slanci locality near Belgrade – in Serbian]. *VII Simpozijum JAM, Mineralogija*, *Godišnjak JAM*, 42–48.

Taylor, J.C. 1991. Computer Programs for Standard less Quan- titative Analysis of Minerals Using the Full Powder Diffraction Profile. *Powder Diffraction*, 6: 2–9.

Toljić, M., Nenadić, D., Stojadinović, U., Gaudényi, T. & Bogićević, K. 2014. Quaternary tectonic and depositional evolution of eastern Srem (northwest Serbia). *Geološki anali Balkanskoga poluostrva*, 75: 43–57.

Van der Made, J., Knežević, S. & Stefanović, I. 2007. A mid-Miocene age for the Slanci formation near Belgrade (Serbia), based on a record of the primitive antelope Eotragus cf. clavatus from Višnjica. *Geološki Anali Balkanskog Poluostrva,* 68: 53–59.

Vujaković, A., Daković, A., Lemić, J., Radosavljević-Mihajlović, A., Tomašević-Čanović, M. 2003. Adsorption of inorganic anionic contaminants on surfactant Singkemodifed minerals. *Journal of the Serbian Chemical Society*, 68 (11): 833–841.

Yang, P. & Armbruster, T. 1996. Na, K, Rb and Cs Exschange in Heulandite Single-Crystal: X-Ray Structure Refinements at 100 K. *Journal of Solid State Chemistry*, 123: 140–149.

Резиме

Минералошка и структурна карактеризација зеолитског туфа лежишта Сланци – Србија

Наслаге језерског миоцена, које се налазе источно од Београда у Дунавском кључу, око Великог Села и Сланаца, изузетно су богате зеолитским туфовима хејландитског типа. Квантитативном рендгенском анализом на прашкастом узорку, утврђен је следећи минерални састав: хејландит (85,1%), кварц (1,9%), мусковит (5,9%), албит (6,6%), ортоклас (0,6%) и калцит (0,21%). Пратеће компоненте су вулканско стакло и биоегена аморфна силикатна маса. На основу хемијских и термичких анализа утврђено је да је доминантна зеолитска фаза Ca-хејландит са одно-сом Si/Al 3,78. Микроскопском анализом утврђено је да је основна маса хипокристаласто порфирска, делимично је шупљикава и порозна. Кварц је редовно свеж, типичних анхедралних форми и оштрих ивица. Честе су гасно-течне-чврсте инклузије. Од минерала фелдспата се јављају углавном плагиокласи, веома често алтерисани серицитисани и делимично каолинисани. Од минерала лискуна доминантан је биотит. Акцесорни минерали су редовно свежи, бистри и без видљивих знакова алтерације – циркон, апатит и рутил. Структура Ca-хејландита је утачњавана у просторној групи $C2/m$, са неуређеном расподелом Al и Si у тетраедарској мрежи. Израчунати параметри јединичне ћелије су a= 17.68 Å; b= 17.924 Å; c= 7.413 Å; β=.116.24°; V= 2117.406 Å^3. Добијени структурни модел за положаје атома (тетраедарских) и катјона у изменљивом положају су у сагласности са литертурним подацима. Одступања која су присутна су у складу са кристалохемијским саставом самог зеолитског туфа. Садржај изменљивих катјона даје капацитет катјонске измене од 160.1, и уз термичку стабилност упућује на могућност коришћења ове сировине у различитим областима индустрије.

Manuscript received October 14, 2025
Revised manuscript accepted November 24, 2025